AD-A055 231 OKLAHOMA STATE UNIV STILLWATER DEPT OF PHYSICS F/G 20/5
MULTISTEP ENERGY MIGRATION AND RADIATIONLESS RELAXATION PROCESS--ETC(U)
MAY 78 R C POWELL DAAG29-76-G-0099
UNCLASSIFIED ARO-1331A.5-P NL

| OF |
AD
A055 231

END
DATE
FILMED
7-78
DDC

Unclassified
SECURITY CLASSIFICATION OF THIS PAGE (When Data Entered)

REPORT DOCUMENTATION PAGE

READ INSTRUCTIONS BEFORE COMPLETING FORM

1. REPORT NUMBER: 13318.5-P	2. GOVT ACCESSION NO.: ARO
3. RECIPIENT'S CATALOG NUMBER:	
4. TITLE (and Subtitle): Multistep Energy Migration and Radiationless Relaxation Processes in Phosphor and Laser Crystals.	5. TYPE OF REPORT & PERIOD COVERED: Technical Report.
	6. PERFORMING ORG. REPORT NUMBER:
7. AUTHOR(s): Richard C. Powell	8. CONTRACT OR GRANT NUMBER(s): DAAG29 76-G-0099
9. PERFORMING ORGANIZATION NAME AND ADDRESS: The Oklahoma State University, Stillwater, Oklahoma 74074	10. PROGRAM ELEMENT, PROJECT, TASK AREA & WORK UNIT NUMBERS: 37p.
11. CONTROLLING OFFICE NAME AND ADDRESS: U. S. Army Research Office, P. O. Box 12211, Research Triangle Park, NC 27709	12. REPORT DATE: 16 May 1978 13. NUMBER OF PAGES: 34
14. MONITORING AGENCY NAME & ADDRESS (if different from Controlling Office)	15. SECURITY CLASS. (of this report): unclassified 15a. DECLASSIFICATION/DOWNGRADING SCHEDULE

16. DISTRIBUTION STATEMENT (of this Report)

Approved for public release; distribution unlimited.

17. DISTRIBUTION STATEMENT (of the abstract entered in Block 20, if different from Report)

18. SUPPLEMENTARY NOTES

The findings in this report are not to be construed as an official Department of the Army position, unless so designated by other authorized documents.

19. KEY WORDS (Continue on reverse side if necessary and identify by block number)

20. ABSTRACT (Continue on reverse side if necessary and identify by block number)

An extensive investigation of the spectroscopic properties of $Nd_xY_{(1-x)}P_5O_{14}$ is reported. Time-resolved site-selection spectroscopy and photoacoustic spectroscopy techniques were used as well as standard optical spectroscopy measurements which were made as a function of Nd concentration, temperature, excitation wavelength and laser power. Results show that Nd ions occupy a variety of slightly perturbed sites. No significant energy transfer appears to be taking place between ions in

400 790

DD FORM 1 JAN 73 1473 EDITION OF 1 NOV 65 IS OBSOLETE

Unclassified
SECURITY CLASSIFICATION OF THIS PAGE (When Data Entered)

20. ABSTRACT CONTINUED

these inequivalent sites. Additional experimental data presented here suggests a new quenching model for neodymium pentaphosphate crystals based on spatial but non-spectral energy migration to surface quenching sites.

MULTISTEP ENERGY MIGRATION AND RADIATIONLESS RELAXATION PROCESSES IN PHOSPHOR AND LASER CRYSTALS

Interim Technical Report

Richard C. Powell

The Oklahoma State University
Department of Physics
Stillwater, Oklahoma 74074

Date Submitted - May 16, 1978

PREPARED FOR THE
UNITED STATES ARMY RESEARCH OFFICE

Army Grant No. DAAG 29-76-G-0099

CONCENTRATION QUENCHING IN $Nd_xY_{1-x}P_5O_{14}$ CRYSTALS

John M. Flaherty* and Richard C. Powell
Department of Physics, Oklahoma State University
Stillwater, Oklahoma 74074

ABSTRACT

An extensive investigation of the spectroscopic properties of $Nd_xY_{1-x}P_5O_{14}$ is reported. Time-resolved site-selection spectroscopy and photoacoustic spectroscopy techniques were used as well as standard optical spectroscopy measurements which were made as a function of Nd concentration, temperature, excitation wavelength and laser power. Results show that Nd ions occupy a variety of slightly perturbed sites. No significant energy transfer appears to be taking place between ions in these inequivalent sites. Additional experimental data presented here suggests a new quenching model for neodymium pentaphosphate crystals based on spatial but non-spectral energy migration to surface quenching sites.

*Present address: GTE-Sylvania Laboratories, Danvers, Mass.

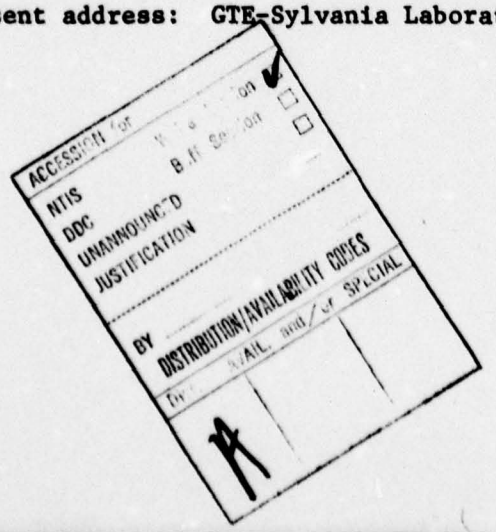

I. INTRODUCTION

The development of the technology of fiber optics has resulted in a requirement for miniature optically pumped lasers with low threshold and high gain.[1] Stoichiometric laser materials such as neodymium pentaphosphate (NdP_5O_{14}) meet these requirements.[2-4] Despite the significant amount of work that has been done recently there are still some aspects of the luminescence properties of concentrated Nd materials which are not well understood. Complete characterization of the optical properties of this class of materials is important not only for technological design considerations but also for obtaining a basic understanding of the physical interaction mechanisms involved.

The most important property of stoichiometric laser materials is that they exhibit unusually weak concentration quenching. This allows the concentration of neodymium ions in NdP_5O_{14} to be very high without significant degradation of the fluorescence and lasing properties of the material. The characteristics of the concentration quenching in stoichiometric laser materials are different from those in other well characterized materials such as $Y_3Al_5O_{12}:Nd^{3+}$ and the physical mechanism for the quenching process is not understood at this time. Developing a model to explain concentration quenching in NdP_5O_{14} is an important problem in understanding this class of materials.

To date three basic mechanisms have been proposed to explain the concentration quenching characteristics of stoichiometric laser materials. All have been proven unsatisfactory. The first mechanism postulated was cross-relaxation between pairs of Nd ions in the bulk of the crystal which predicted a quadratic concentration dependence for the quenching rate[5-8]. This prediction is inconsistent with experimental results.[1-9] A second suggestion for a quenching mechanism involved crystal field overlap mixing effects between Nd^{3+} ions[10] but this has been proved wrong by the observation that the

oscillator strengths of the Nd^{3+} transitions are independent of concentration.[11] Finally energy migration to ions in randomly distributed sites throughout the bulk of the crystal acting as "sinks" where the energy is dissipated radiationlessly has been proposed.[6,7,9,12] Unfortunately this model requires the unrealistic assumption that the concentration of ions in quenching sites is the same for all samples independent of total Nd concentration.[9] We recently reported preliminary results indicating that spectral energy transfer between Nd^{3+} ions in slightly different types of sites is not taking place in NdP_5O_{14} as it does in materials such as $Y_3Al_5O_{12}:Nd^{3+}$ even at low concentrations.[13]

In this paper we report the results of an investigation of the mixed crystal system of $Nd_xY_{1-x}P_5O_{14}$ where we have utilized some new spectroscopic techniques in an attempt to better understand the concentration quenching mechanism in these materials. Laser time-resolved site-selection spectroscopy was used to investigate energy transfer and the results show that migration among Nd^{3+} ions in non-equivalent sites does not take place. Photoacoustic spectroscopy (PAS) measurements were made to characterize radiationless relaxation processes among the excited states of Nd^{3+} in these materials. The results are not consistent with those expected for PAS signals originating mainly from those phonons due to relaxation processes from higher absorption levels to the metastable level. A model based on surface quenching of the excitation is proposed which can explain the observed PAS results and is consistent with all the other spectroscopic observations obtained on this material. The possible mechanisms for the quenching process and the effects of radiative reabsorption are also discussed.

II. SAMPLES AND EXPERIMENTAL EQUIPMENT

The samples were grown from solution at Philips Laboratory. Six samples of $Nd_xY_{1-x}P_5O_{14}$ ranging from x=1.00 to x=0.10 were investigated. These con-

sisted of small crystallites varying in size from about 2.0 mm on a side to about 0.50 mm.

For optical spectroscopy measurements the samples were mounted in a cryogenic refrigerator to control the temperature. For photoacoustic spectroscopy the samples were mounted in an acoustical cavity and the signal detected by a 1-in. electret microphone. The excitation source for obtaining PAS and fluorescence excitation spectra was a 1000-W tungsten/halogen lamp passed through a 1/4-m monochromator. For measuring fluorescence lifetimes and obtaining time-resolved spectroscopy data the excitation source was a nitrogen laser-pumped tunable dye laser with rhodamine 6-G dye. This provided a pulse of about 10 ns in duration and less than 0.5 Å in halfwidth. Sample emission was analyzed by a one-meter monochromator and detected by a cooled RCA C31034 photomultiplier tube. To obtain steady state spectral data the incident light was chopped and the signal processed by a PAR lock-in amplifier. For processing pulsed signals a PAR boxcar averager triggered by the laser pulse was used. The time gate of the boxcar was either set to observe the fluorescence spectrum at a specific time after the laser pulse or scanned to obtain the fluorescence as a function of time at a specific wavelength.

Figure 1 shows block diagrams of the experimental setups for time-resolved spectroscopy and photoacoustic spectroscopy measurements.

III. GENERAL SPECTROSCOPY AND CONCENTRATION QUENCHING RESULTS

The absorption spectrum of NdP_5O_{14} has been presented elsewhere.[1] It is similar to the spectrum of Nd^{3+} ions in other hosts with lower doping concentrations. The largest absorption band occurs at approximately 8000 Å corresponding to the transition from the $^4I_{9/2}$ ground state to a band consisting of the unresolved components of the $^2H_{9/2}$ and $^4F_{5/2}$ levels (see the energy diagram of Nd^{3+} shown in Fig. 2). The second largest absorption band occurs near 5800 Å and is associated with the unresolved levels of the $^2G_{7/2}$ and

$^4G_{5/2}$ levels. After absorption into any of the higher energy levels, radiationless relaxation occurs to the $^4F_{3/2}$ metastable state. Fluorescence emission then takes place from the two crystal field components of this level to the various Stark components of the ^4I_J multiplets. Branching ratios determined previously[7] indicate that most of the energy is emitted in the transitions terminating on the $^4I_{11/2}$ and $^4I_{9/2}$ levels centered around 1.06 μm and 0.89μm, respectively. The fluorescence spectrum is discussed in more detail in the next section.

Figure 3 shows the fluorescence excitation spectra of the $^4F_{3/2}$ level monitored at 8880 Å at room temperature for both NdP_5O_{14} and a mixed crystal of $Nd_{0.5}Y_{0.5}P_5O_{14}$. The spectra are quite similar for the pure and mixed samples. In particular, the excitation bands centered at ~ 8000 Å and ~ 5800 Å are comparable. The relative strength in the absorption spectrum of these two bands[1] correlated with the fact that the 8000 Å excitation is approximately the same or less intense than the 5800 Å band in the excitation spectrum suggests that the longer wavelength band is less efficient in contributing to $^4F_{3/2}$ fluorescence than the shorter wavelength band.

Figure 4 shows the fluorescence lifetime of the $^4F_{3/2}$ level at room temperature as a function of Nd concentration. The lifetime decreases from about 220 μs for the $Nd_{0.1}Y_{0.9}P_5O_{14}$ sample to about 95 μs for NdP_5O_{14}. A concentration quenching rate can be defined as

$$W_Q = \tau^{-1} - \tau_o^{-1} \qquad (1)$$

where τ_o is the Nd fluorescence lifetime in the absence of any quenching interaction. This quenching rate is also plotted in Fig. 4 as a function of concentration. For an intrinsic lifetime of ~ 220 μs the plot of the quenching rate appears to vary approximately linearly with concentration.

The fluorescence lifetime of the $^4F_{3/2}$ level was measured with different wavelengths of excitation as a function of temperature between 14 K and 300 K.

The fact that a significant variation in lifetime with excitation wavelength was observed is discussed in the next section. The temperature dependence of the fluorescence lifetime for NdP_5O_{14} for two different wavelengths of excitation is shown in Fig. 5. There is a small increase in lifetime between 14 and 300 K. A similar trend is observed for other samples and other excitation wavelengths.

IV. TIME-RESOLVED SITE-SELECTION SPECTROSCOPY RESULTS

The optical spectral lines of impurity ions in solids all exhibit inhomogeneous broadening to some degree. This is due to the fact that imperfections and internal strains give rise to non-equivalent crystal field sites for the impurity ions. In some cases the site differences are great enough that transitions from ions in different types of sites can be distinctly resolved. High resolution lasers have been used to selectively excite impurity ions in specific crystal field sites in glass and crystal hosts. By tuning the laser excitation through an inhomogeneously broadened absorption band it has been possible to observe significant variations in fluorescence spectral parameters such as peak positions, intensities, and radiative and radiationless transition probabilities.[14] If pulsed lasers are used, time-resolved spectroscopy techniques allow the observation of the fluorescence spectrum at specific times after the laser pulse. After selective excitation of ions in specific sites the fluorescence spectrum in some systems has been observed to evolve with time into spectra exhibited by ions in other types of sites. This implies that energy transfer is occurring between ions in different types of sites and the observed time dependence can be used to characterize the properties of the energy transfer and help in identifying the mechanism responsible for the transfer process.

For investigating site selection spectroscopy in the $Nd_xY_{1-x}P_5O_{14}$ system we pumped into the absorption band consisting of the unresolved $^2G_{7/2}$ and

$^4G_{5/2}$ levels because this transition is known to be "hypersensitive" to changes in the local environment of the ion 11,15,16 and for other systems such as Nd in mixed garnet crystals we found that pumping into this level resulted in easily observable site-selection and energy transfer.[17] The fluorescence was monitored from the $^4F_{3/2}$ level to the various components of the $^4I_{9/2}$ ground state manifold in order to minimize homegeneous broadening of the transitions due to radiationless relaxation processes. As the narrow line laser excitation was scanned across the broad absorption band at low temperatures, for all of the samples investigated, changes in the relative fluorescence peak intensities, peak positions, and lifetimes were observed. For example, for the NdP_5O_{14} sample at 14 K the lifetimes ranged from 63μs to 105 μs depending on the excitation wavelength whereas at 300 K they varied between about 102 and 115 μs. Figure 6 shows an example of the different fluorescence spectra which are obtained for the NdP_5O_{14} sample at 14 K for pumping at different wavelengths. The total integrated intensity of the fluorescence is approximately the same for each excitation wavelength but the distribution of the intensity among the five lines and the fluorescence lifetimes differ significantly. The lifetime is 67 μs for 5784.5 Å excitation and 77 μs for 5837 Å excitation. The highest energy line (labeled 1 in the figure) shows the greatest variation with pumping wavelength but there are relative changes in the intensities of all of the other lines also. Figure 7 shows an expanded picture of line 1 as a function of excitation wavelength at 14 K for the $Nd_{0.5}Y_{0.5}P_5O_{14}$ crystal. Here the changes in line shape and peak position are quite evident. For the 5831 Å excitation the line is resolved into two distinct peaks.

These spectral as well as lifetime changes as a function of excitation wavelength can be attributed to the selective excitation of Nd ions in non-equivalent crystal field sites. If rapid energy migration occurs among the

Nd ions the spectra should evolve with time into some characteristic spectrum representing the average distribution of the energy among all of the ions in different types of sites. We attempted to observe this by monitoring the spectra as a function of time after the laser pulse in the range from 1 to 200 μs. No significant time evolution of the spectra was detected in this range for either of the two samples investigated, NdP_5O_{14} and $Nd_{0.5}Y_{0.5}P_5O_{14}$, for any wavelength of excitation at any temperature.

In order to quantitatively describe any time dependent relative changes in the spectra obtained for two different excitation wavelengths a fluorescence deviation function can be defined. The spectrum obtained for a given excitation wavelength is represented by a five component function each component corresponding to the ratio of the integrated intensity of one of the lines of the $^4F_{3/2} \rightarrow {}^4I_{9/2}$ transitions to the total integrated intensity of all of the lines. Thus each fluorescence spectrum can be characterized by a five component vector. Any correlation between the fluorescence spectra for different excitation wavelengths can be seen by forming the vector difference between the functions describing the spectra for each excitation wavelength. Figure 8 shows typical results for the fluorescence deviation as a function of time after the laser pulse for both the NdP_5O_{14} sample and the $Nd_{0.5}Y_{0.5}P_5O_{14}$ at various temperatures. A value of D equal to 0 would indicate an identical distribution of relative intensities in the five spectral lines for the two excitation wavelengths. The presence of energy transfer between Nd ions in different types of sites should result in a time dependent decrease in D toward zero. Instead for all cases investigated D remains within experimental error constant with time indicating that no energy transfer is taking place between ions in non-equivalent sites.

The temperature dependence of the fluorescence deviation function for NdP_5O_{14} is shown in Fig. 9. The error bars indicate the spread in the values

of D for measurements at different times after the laser pulse at each temperature. Since the decrease in D with temperature occurs without any associated time dependence, this temperature dependence can be attributed to the reduced ability of the laser to selectively excite Nd ions in specific sites at high temperatures. This may be a result of homogeneous broadening of the absorption levels due to electron-phonon interactions.

The site-selection spectroscopy results presented above show that Nd ions in pentaphosphate hosts occupy different types of crystal field sites. Although the exact nature of these different sites is not known they are probably due to differences in local strains resulting from structural imperfections and defects in the crystal. The similar relative intensities observed for different excitation wavelengths imply similar concentrations for the different types of sites. The fact that no energy transfer could be detected between ions in different types of sites is quite surprising in light of the fact that similar studies made on Nd ions in mixed garnet crystals show strong energy transfer between ions in non-equivalent sites.[17] It is important to note however that spatial energy transfer between Nd ions in equivalent sites may take place without spectral energy transfer to ions in different types of sites. This type of transfer would not be observable by the time-resolved site-selection spectroscopy techniques used here and is discussed further in Sections 6 and 7.

V. PHOTOACOUSTIC SPECTROSCOPY RESULTS

Photoacoustic spectroscopy techniques have recently been developed to characterize radiationless decay processes of ions in crystals.[18-21] By comparing PAS results with fluorescence excitation spectra it has been possible to determine dominant relaxation channels.[20,21] Low resolution photoacoustic spectra were obtained at room temperature on the concentrated neodymium pentaphosphate samples. The 1000 W tungston-halogen lamp chopped at 110 Hz

was used as an excitation source. Figure 10 shows the results obtained on the NdP_5O_{14} sample and the $Nd_{0.9}Y_{0.1}P_5O_{14}$. The signal to noise ratio on the more lightly doped samples was too poor to give meaningful results. Note that the relative peak heights of the major absorption bands in the PAS spectrum are comparable to those in the absorption and excitation spectra.

These PAS results are more difficult to interpret than those in the previous samples investigated.[20-21] The photoacoustic signal normalized for the energy of the incident light beam at phase angle Θ can be expressed as the sum over all the relaxation transitions which generate heat[20]

$$I_{PAS}(\Theta) \propto N_a \sum_i \phi_{nr}(i) h\nu_i \cos(\alpha_i - \Theta)/(N_o h\nu_o) \qquad (2)$$

where N_a is the number of photons absorbed, $\phi_{nr}(i)$ is the fraction of excited atoms relaxing via the ith type of radiationless transition, $h\nu_i$ is the energy of the phonons emitted in the ith process, and α_i is the phase angle at which the signal due to transitions from the initial state of the ith transition is maximum. N_o and $h\nu_o$ are the number and energy of the photons in the excitation beam. For the case of Nd^{3+} ions the sum in Eq. (2) should include three different types of radiationless decay processes which occur during the relaxation of the ion from the level excited by the incident light. First, phonons will be emitted during the decay from the absorption state to the $^4F_{3/2}$ metastable level. Second, the $^4F_{3/2}$ level does not have unit radiative quantum efficiency and thus some amount of relaxation from this state to the ground state occurs radiationlessly. Third, the majority of the fluorescence transitions from the $^4F_{3/2}$ state terminate on levels of the ^4I_J multiplets other than the ground state and subsequent relaxation to the ground state occurs radiationlessly. Previous measurements have shown that there is virtually unit probability of relaxing to the metastable level after pumping into higher excited states.[22]. The radiative quantum efficiency of the $^4F_{3/2}$ level is of the order of ~0.9 in the absence of quenching interactions.[23] Most of the emission terminates on

either the $^4I_{11/2}$ or the $^4I_{9/2}$ multiplets. Thus from these considerations and the energy level diagram shown in Fig. 2, it would seem that the higher lying absorption bands should be more intense in the PAS spectrum compared to the lower energy bands than in the absorption and excitation spectra due to the first type of decay processes listed above. This is the type of behavior observed in other samples.[20,21] Figure 10 shows that this is not the case here as exemplified by the fact that the 8000 Å band is equal or greater in intensity than the 5800 Å band.

This comparison of the absorption, excitation, and photoacoustic spectra indicates that there is relatively more radiationless quenching occurring after excitation into the 8000 Å band than after excitation into the 5800 Å band. Since the absorption coefficients of these two bands are different, a different spatial distribution of excited ions will occur after excitation into each band. For such heavily concentrated systems as those considered here, the high absorption coefficient of the 8000 Å band will result in a significant fraction of the excited Nd ions being located close to the surface of the crystal. The somewhat smaller absorption coefficient for the 5800 Å band allows for more of the excited ions to be located farther into the bulk of the crystal. One mechanism to explain the spectral properties reported here is surface quenching which is discussed in detail in the next section.

VI. INTERPRETATION OF RESULTS

At this point it is worthwhile to summarize the experimental observations which must be explained by any viable model of concentration quenching in $Nd_xY_{1-x}P_5O_{14}$ and similar materials. The quenching rate must vary linearly with Nd concentration. Also it must have a very weak dependence on temperature and it must be proportional to the absorption cross section. The quenching mechanism cannot lead to variations in oscillator strengths with Nd concentration, cannot result in spectral energy transfer, and cannot lead to

non-exponential fluorescence decays. These requirements along with quantitative theoretical predictions place very rigid restrictions on developing an acceptable model for concentration quenching in these materials. The mechanism responsible for concentration quenching of Nd fluorescence in other types of materials such as $Y_3Al_5O_{12}:Nd^{3+}$ is cross-relaxation between pairs of closely spaced ions. This leads to a quadratic dependence of the quenching rate on Nd concentration which is contrary to the linear dependence observed for the pentaphosphate hosts. The other common mechanism for concentration quenching which is observed in various materials is migration of the energy among the active ions until it reaches a sink where it is transferred to an ion which can dissipate the energy radiationlessly. This mechanism is not consistent with several of the requirements mentioned above. There is no dependence of the quenching rate on absorption cross section in this model and generally quenching by this mechanism has been found to lead to a strong temperature dependence. A quantitative estimate of the concentration of sinks necessary to give the observed quenching rate can be obtained in the fast diffusion limit from the expression $W_Q=4\pi DR_sC_s$ where D is the diffusion coefficient, R_s is the exciton trapping radius at the sink, and C_s is the sink concentration. For the case of neodymium pentaphosphate a sink concentration of only 10 ppm of the Nd ions is necessary to cause the observed quenching rate whereas site-selection spectroscopy shows that significant numbers of Nd ions exist in sites of different local perturbations without resulting in energy transfer or quenching.

Since the normal models for concentration quenching do not appear to apply to stochiometric laser materials it is necessary to develop a new model. One model which appears to meet all of the requirements outlined above is based primarily on surface quenching of the excitation energy. In this model the Nd ions on the surface of the sample act as sinks where the energy is dissipated

radiationlessly. This gives a high concentration of sink sites but only in a very small region and not distributed uniformly throughout the sample. This situation will result in effective quenching for concentrated materials where the excitation energy is deposited near to the sample surface whereas it will be much less effective in lightly doped materials where the energy is deposited more uniformly throughout the sample. Similarly for a given sample quenching will be more effective where the absorption of exciting light is stronger due to the fact that more of the excited ions will reside closer to the surface. Weaker absorption bands will allow excitation energy to be deposited further into the crystal resulting in less effective quenching.

To determine whether or not a surface quenching model satisfies all of the necessary requirements for explaining the observed data, an expression for the quenching rate can be derived from simple geometric arguments based on the situation shown in Fig. 11. The incident light excites a Nd ions at a distance R from the surface of the crystal and the energy can as an exciton migrate out from this site to other Nd ions. According to standard diffusion theory, after a time equal to the intrinsic lifetime of the exciton the excitation energy will be found on one of the ions on the surface of a sphere of radius ℓ centered at the position of the originally excited ion. ℓ is the diffusion length which is determined by

$$\ell = \sqrt{6 D \tau_o} \tag{3}$$

where τ_o is the intrinsic lifetime of the exciton. If it is assumed that only excitons which migrate far enough to reach the surface are quenched, the quenching rate for an excited ion at depth R is

$$\begin{aligned} W_Q(R) &= p\tau_o^{-1}(A'/A) && 0 \leq R \leq \ell \\ W_Q(R) &= 0 && \ell < R \end{aligned} \tag{4}$$

where A is the area of the sphere of radius ℓ, A' is the part of the area of this sphere which is outside the sample surface, and p is a factor to account

for the probability of energy being dissipated radiationlessly instead of radiatively when it reaches the surface. The fraction of the area outside the sample can be found from the double integration

$$A = 2\ell\int_0^{\phi_M} d\phi 2\ell\int_{\theta_m}^{\pi/2} \sin\theta d\theta$$
$$= 4\ell\sqrt{\ell^2-R^2}\cos^{-1}(R/\ell). \quad (5)$$

Thus the first part of Eq. (4) becomes

$$W_Q(R) = p(\tau_o\pi\ell)^{-1}\sqrt{\ell^2-R^2}\cos^{-1}(R/\ell) \quad 0\leq R\leq\ell \quad (6)$$

The observed fluorescence intensity is proportional to the concentration of excited ions. At time t the remaining concentration of excited ions which were originally created at a depth R into the sample is given by the product of the probability of exciting an ion at that position multiplied by the exponential decay function for such ions

$$n_R^*(t) = \exp\left[-t(\tau_o^{-1}+W_Q(R))\right] I_o\sigma C\exp-\sigma CR\, dR \quad (7)$$

Here C is the concentration of Nd ions and σ is the absorption cross section and I_o is the intensity of the incident light. The total concentration of excited Nd ions is found by integrating this expression over the entire thickness of the crystal T. Using Eqs. (4) and (6) this becomes

$$n^*(t) = \sigma C I_0 e^{-t/\tau_0}\left[\int_0^{\ell}\exp\left[-tp(\tau_o\pi)^{-1}\sqrt{1-(R-\ell)^2}\cos^{-1}(R/\ell)\right]dR + \int_{\ell}^{T}\exp\left[-\sigma CR\right]dR. \quad (8)$$

Evaluation of this expression shows that in this model the time dependence of the fluorescence intensity is described by

$$I(t) = I(0)\exp\left[-t(\tau_o^{-1} + 0.226p\sigma C\ell\tau_o^{-1})\right] \quad (9)$$

Thus the quenching rate is given by

$$W_Q = 0.226p\sigma C\ell\tau_o^{-1} \quad (10)$$

The results of these considerations show that a surface quenching model predicts exponential fluorescence decays and a quenching rate which varies linearly with both Nd concentration and absorption cross section. Since the

ion-ion interaction responsible for the migration is a resonant interaction, no thermal activation is necessary and only a weak temperature dependence is expected. The quenching rate should actually be somewhat greater at low temperatures where there is less phonon scattering to limit the mean free path of the exciton. This appears to be verified by the lifetime data shown in Fig. 5. Quantitatively the experimentally observed quenching rate for neodymium pentaphosphate can be predicted by Eq. (10) if the thermal conversion probability for excitons reaching the surface (p) is taken to be unity and the diffusion length is of the order of 3,600 Å. Previous estimates of the diffusion length of excitons in this material have ranged from 360 to 5,000 Å. A theoretical estimate for the diffusion coefficient can be obtained from the expression

$$D = \frac{1}{6} R_{nn}^2 \tau_H^{-1} \tag{11}$$

A rough estimate of the hopping rate between two Nd ions separated by a distance R_{nn} can be found by assuming a nearest neighbor electric dipole-dipole interaction for two ions in exact resonance

$$t_H^{-1} = W_{Nd\text{-}Nd} = \tau_0^{-1}(R_0/R_{nn})^6 \tag{12}$$

where the critical interaction distance R_0 is given by

$$R_0 = \left[\frac{3e^4 f^2 \Omega \tau_0}{8\pi^2 m^2 c^2 n^4 \bar{\nu}}\right]^{\frac{1}{6}} \tag{13}$$

Here f is the oscillator strength of the transition between the ground and metastable state. $\bar{\nu}$ is the average wavenumber in the region of spectral overlap, and Ω is the spectral overlap integral. For two overlapping Lorentzian lines

$$\Omega = \frac{1}{\pi} \frac{\Delta\nu_1 + \Delta\nu_2}{(\Delta\nu_1 + \Delta\nu_2)^2 + (\nu_1^o + \nu_1 + \nu_2^o)^2} \tag{14}$$

where ν^o is the peak position and $\Delta\nu$ is the Lorentzian contribution to the line width. Thus for perfect overlap Ω is proportional to the inverse of the homogeneous contribution to the spectral line width. This is measured at low

temperatures to be about 6 cm^{-1}. This can be used in Eq. (13) which leads to a predicted value of 54 Å for R_0. Then for a nearest neighbor distance of 5.6 Å Eq. (12) predicts an ion-ion interaction rate of 3.65×10^9 sec^{-1}. Substituting these numbers into Eq. (11) yields a predicted diffusion coefficient of 1.9×10^{-6} cm^2 sec^{-1}. Then substituting this result into Eq. (3) gives a predicted diffusion length of about 5,000 Å which is consistent with the value needed to interpret the concentration quenching data with a surface quenching model.

An attempt was also made to fit the data with a surface quenching model in which the excitation energy did not diffuse but rather was transferred to the surface ions in a single step electric dipole-dipole process. The predictions of this model were not consistent with the observed results because they predicted a non-exponential decay time and quantitatively an unphysically large value for the interaction strength had to be assumed to give the correct magnitude for the quenching rate.

A direct check was made on the prediction that the quenching rate is proportional to the absorption cross section by monitoring the fluorescence lifetime as the laser excitation was scanned from the peak to the wings of the absorption band. The results obtained at 14 K for the NdP_5O_{14} sample are shown in Fig. 12. There is an obvious increase in fluorescence lifetime and thus a decrease in the quenching rate as the excitation is scanned from the region of high absorption to one of small absorption as predicted. However the dependence of W_Q on σ appears to be less than the linear dependence predicted by Eq. (10). There may be several reasons for this. First it is difficult to change the laser wavelength without also altering its power and beam position. Thus it is impossible to exactly repeat the experimental conditions from point to point in Fig. 12 and only the general trend of the data can be considered important. Also the theoretical derivation of Eq. (10) is based

on the assumption that the number of photons absorbed from the incident beam at depth R is directly proportional to the absorption cross section. This is only true for small values of the absorption coefficient. The exact expression is

$$\begin{aligned} n &= n_0 \left[1-\exp(-\sigma CR)\right] \\ &= n_0 \sigma CR \left[1-\tfrac{1}{2}\sigma CR+\tfrac{1}{6}(\sigma CR)^2-\ldots\right] \end{aligned} \tag{15}$$

and thus for the high optical densities treated here the variation with absorption cross section should be less than linear. The linear approximation was made in deriving Eq. (10) only to simplify the calculations.

There is still a question as to the exact mechanism for quenching after the exciton has migrated to the surface. The energy levels of the surface ions may be perturbed in such a way that they act as sinks or allow for cross-relaxation to occur with other Nd ions. A third possibility is that there is such a high density of excited Nd ions on the surface that bi-excitonic processes are responsible for the quenching. The latter possibility was investigated by monitoring the fluorescence lifetime as a function of laser power for the NdP_5O_{14} sample at 14 K. The excitation was near the peak of the 5800 Å band and the power was decreased by a set of calibrated neutral density filters. The fluorescence lifetime was found to increase slightly with decreased laser intensity. This suggests that some amount of exciton-exciton interaction may be taking place. However the dependence of W_Q on laser power does not appear to be strong enough to account for all of the quenching and most probably several different mechanisms are taking place at the same time.

VII. DISCUSSION AND CONCLUSIONS

The surface quenching model described in the preceeding section is consistent with all of the results obtained in this investigation. It also appears

to be consistent with data reported by other workers. Similar surface quenching effects have also been observed in other types of materials with high absorption coefficients such as aromatic hydrocarbon crystals.[24]

For crystals with high absorption coefficients radiative reabsorption effects should be expected. We attempted to determine the extent of such effects by observing the fluorescence lifetime as a function of sample alignment. The lifetime appeared to lengthen slightly in going from front face to back face illumination. All data reported here were obtained with front face illumination to minimize radiative reabsorption effects.

It should be pointed out that there is a possible alternative explanation for the fact that the relaxation processes in the excited states do not appear to contribute to the PAS signal. This would be true if the decay occurred radiatively instead of radiationlessly. There has been some weak fluorescence observed between 1.4 and 1.7 μm which has not been explained.[7] However this was observed only at a high level of excitation and only at room temperature and thus can not generally account for all of the observed quenching characteristics.

It is still not clear exactly why the fluorescence quenching rate is so much less in NdP_5O_{14} than in YAG:Nd. One obvious difference is that there is less resonance between the $^4F_{3/2} \rightarrow {}^4I_{15/2}$ emission transitions and the $^4I_{9/2} \rightarrow {}^4I_{15/2}$ absorption. Also a distinguishing feature of the pentaphosphate host is that the Nd ions are fairly isolated from each other and do not share the same oxygen ion.[4] Another interesting observation is that the quenching of Nd fluorescence in phosphate glass hosts is also significantly less than for other glasses.[25] Which of these features is most important in determining the quenching characteristics is not evident. It is known that hydrogen and other impurity ions are very effective in quenching the fluorescence in these materials.[26] These impurities may perturb the energy levels of neighboring Nd ions to allow stronger quenching interactions to occur. The energy levels of surface ions may similarly be perturbed.

interactions to occur. The energy levels of surface ions may similarly be perturbed.

The numerical factors in Eq. (3) and (11) are exact for isotropic random walks on a cubic lattice. These will be slightly different for the pentaphosphate lattice structure but the cubic lattice approximation is sufficient for the order of magnitude estimates needed here.

The diffusion coefficient of the order of $\sim 10^{-6}$ cm^2 sec^{-1} determined for NdP_5O_{14} is significantly greater than the typical values of D which range between 10^{-9} to 10^{-14} cm^2 sec^{-1} for energy migration among other systems of rare earth ions in solids.[27] The reason for this is primarily the higher concentration of Nd ions. This results in efficient spatial diffusion without spectral diffusion. As the excitation energy migrates near to a spectrally different site there are always a significant number of ions nearby in equivalent sites that favor transfer. Only at the surface is there a significant concentration of perturbed ions to cause effective quenching.

In summary the results of time-resolved site selection spectroscopy, photoacoustic spectroscopy, and other investigations presented here are consistent with a model involving spatial energy migration without spectral diffusion which results in significant radiationless quenching at the surface.

ACKNOWLEDGEMENTS: The authors gratefully acknowledge the information supplied by M.J. Weber concerning quenching in phosphate glass hosts, discussions with M.G. Rockley on photoacoustic spectroscopy, and J.G. Gualtieri for suggesting this problem and supplying us with the samples. This work was supported by the U.S. Army Research Office.

REFERENCES

1. S.R. Chinn, H. Y-P. Hong and J.W. Pierce, Laser Focus 12.(May), 64 (1976).
2. H.G. Danielmeyer and H.P. Weber, IEEE J. Quantum Elect. 8, 805 (1972).
3. H.G. Danielmeyer, in Festkörperprobleme (Advances in Solid State Physics), ed H.J. Quiesser (Pergamon/Vieweg, Braunschweig, 1975) vol. 15, p. 253.
4. H.P. Weber, Opt. and Quantum Elect. 7. 431 (1975).
5. S. Singh, D.C. Miller, J.R. Potopowicz and L.K. Shick, J. Appl. Phys. 46. 1191 (1975).
6. W. Strek, C. Szafranski, E. Lukowiak, Z. Mazurak and B. Jezowska-Trzebiatowska, Phys. Stat. Sol. A 41, 547 (1977).
7. M. Blätte, H.G. Danielmeyer, and R. Ulrich, Appl. Phys. 1, 275 (1973).
8. B.C. Tofield, H.P. Weber, T.C. Damen and P.F. Liao, J. Solid State Chem. 12, 207 (1975).
9. A. Lempicki, Optics Comm. 23, 376 (1977).
10. H.G. Danielmeyer, J. Lumin. 12/13, 179 (1976).
11. F. Auzel, IEEE J. Quantum Elect. 12, 258 (1976).
12. P.P. Liao, H.P. Weber, and B.C. Tofield, Solid State Comm. 16, 881 (1973).
13. J.M. Flaherty and R.C. Powell. Solid State. Comm., to be published. (1978).
14. C. Brecher, L.A. Riseberg, and M.J. Weber. Appl. Phys. Lett. 30, 475 (1977); C. Brecher and L.A. Riseberg, Phys. Rev. B 13, 81 (1976); M.D. Kurz and J.C. Wright, J. Lumin. 15, 169 (1977); R.K. Watts and W.C. Holton, J. Appl. Phys. 45, 873 (1974); C. Hsu and R.C. Powell, Phys. Rev. Letters 35, 734 (1975); C. Hsu and R.C. Powell, J. Phys. C 9, 2467 (1976); G.E. Venikouas and R.C. Powell, Phys. Rev. B, to be published, (1978); R. Flach, D.S. Hamilton, P.S. Selzer, and W.M. Yen, Phys. Rev. B 15, 2348 (1977); P.M. Selzer, D.S. Hamilton and W.M. Yen, Phys. Rev. Letters 38, 858 (1977); J. Koo, L.R. Walker, and S. Geschwind,

Phys. Rev. Letters 35, 1669 (1975); and N. Motegi and S. Shionoya, J. Luminescence 8, 1 (1973).

15. F. Auzel, Ann. Telecommun. 24, 199 (1969).
16. B.R. Judd, Phys. Rev. 127, 750 (1962).
17. M. Zokai and R.C. Powell, Bull. American Phys. Soc. 23, 202 (1978).
18. A. Rosencwaig, Opt. Commun. 7, 305 (1973); Anal. Chem. 47, 593 (1975).
19. J.C. Murphy and L.C. Aamodt, J. Appl. Phys. 48, 3502 (1977).
20. L.D. Merkle and R.C. Powell, Chem. Phys. Letters 46, 303 (1977).
21. R.G. Peterson and R.C. Powell, Chem. Phys. Letters 53, 366 (1978).
22. H.P. Weber and B.C. Tofield, IEEE J. Quantum Elect. 11, 368 (1975).
23. H.P. Weber, P.F. Liao and B.C. Tofield, IEEE J. Quantum Elect. 10, 563 (1974).
24. R.C. Powell and Z.G. Soos, J. Luminescence 11, 1 (1975).
25. M.J. Weber, private communications.
26. B.C. Tofield, H.P. Weber, T.C. Damen and G.A. Basteur, Mat. Res. Bull. 9, 435 (1974).
27. R.K. Watts, in "Optical Properties of Ions in Solids", edited by B. DiBartolo (Plenum Press, New York, 1975).

FIGURE CAPTIONS

Figure 1. A) Block diagram of time-resolved spectroscopy setup
B) Block diagram of photoacoustic spectroscopy setup

Figure 2. Energy level scheme of Nd^{3+}

Figure 3. Excitation Spectrum of $^4F_{3/2}$ level in $Nd_{0.5}Y_{0.5}P_5O_{14}$ and NdP_5O_{14} at 300 K.

Figure 4. Concentration dependence of the $^4F_{3/2}$ fluorescence lifetime and quenching rate for $Nd_xY_{1-x}P_5O_{14}$ at 14 K

Figure 5. Temperature dependence of the fluorescence lifetime of the $^4F_{3/2}$ level in NdP_5O_{14} for laser excitation wavelengths of 5804 Å and 5836 Å

Figure 6. $^4F_{3/2} \rightarrow {}^4I_{9/2}$ fluorescence in NdP_5O_{14} 20 μs after selective excitation into different regions of the $^2G_{7/2}$, $^4G_{5/2}$ absorption band at 14 K

Figure 7. Line 1 of $^4F_{3/2} \rightarrow {}^4I_{9/2}$ fluorescence in $Nd_{0.5}Y_{0.5}P_5O_{14}$ after 20 μs excitation at various wavelengths.

Figure 8. A) Time dependence of the fluorescence deviation function after excitation at 5784.5 Å and 5837 Å in NdP_5O_{14} for temperatures 14, 42, 75 and 110 K
B) Time dependence of the fluorescence deviation function after excitation at 5805.5 Å and 5835 Å in $Nd_{0.5}Y_{0.5}P_5O_{14}$ for temperatures 14 and 77 K

Figure 9. Temperature dependence of the fluorescence duration function after excitation at 5784.5 Å and 5837 Å in NdP_5O_{14}

Figure 10. Photoacoustic Spectra of $Nd_{0.9}Y_{0.1}P_5O_{14}$ and NdP_5O_{14} at 300 K

Figure 11. Top and side view geometry for excitation energy migration in surface quenching model.

Figure 12. $^4F_{3/2}$ fluorescence lifetime vs. wavelength of laser excitation at 14 K along with laser probed absorption band at 300 K for NdP_5O_{14}

A

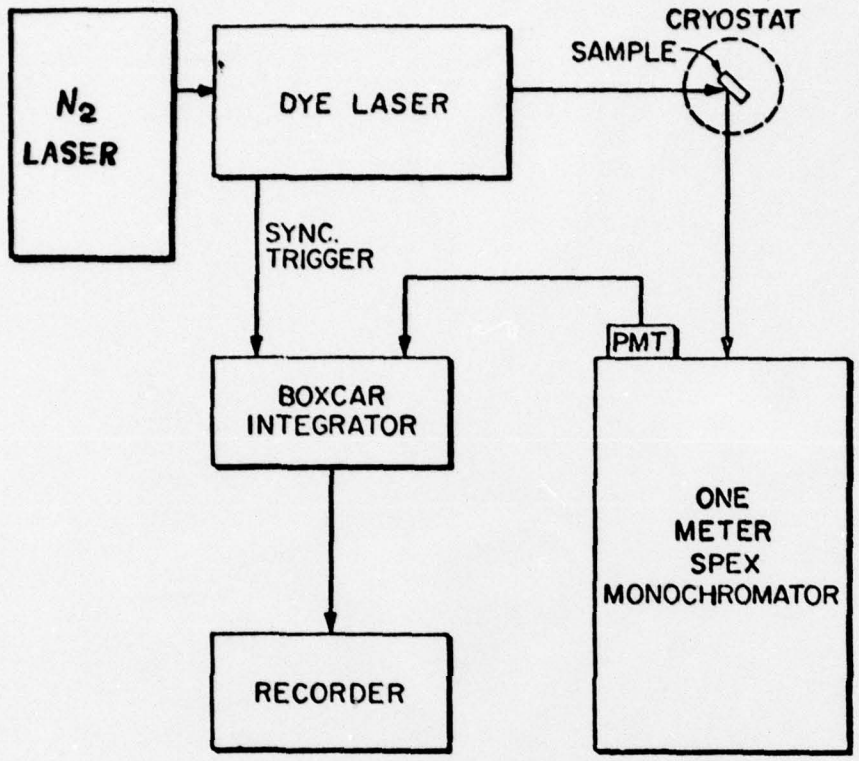
N_2 LASER
DYE LASER
CRYOSTAT
SAMPLE
SYNC. TRIGGER
PMT
BOXCAR INTEGRATOR
ONE METER SPEX MONOCHROMATOR
RECORDER

B

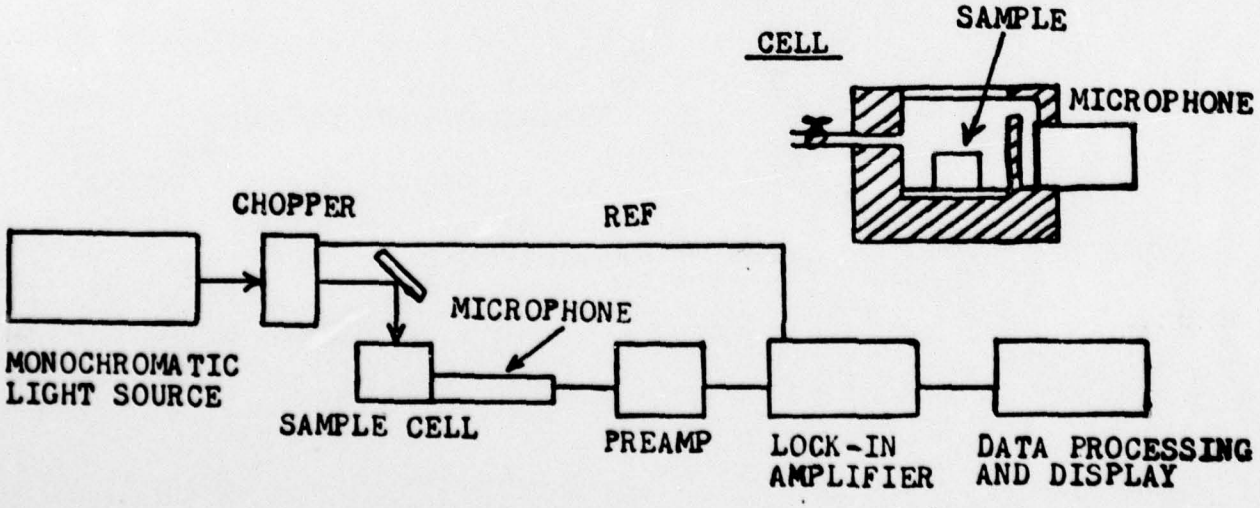
CELL
SAMPLE
MICROPHONE
CHOPPER
REF
MICROPHONE
MONOCHROMATIC LIGHT SOURCE
SAMPLE CELL
PREAMP
LOCK-IN AMPLIFIER
DATA PROCESSING AND DISPLAY

Fig. 1

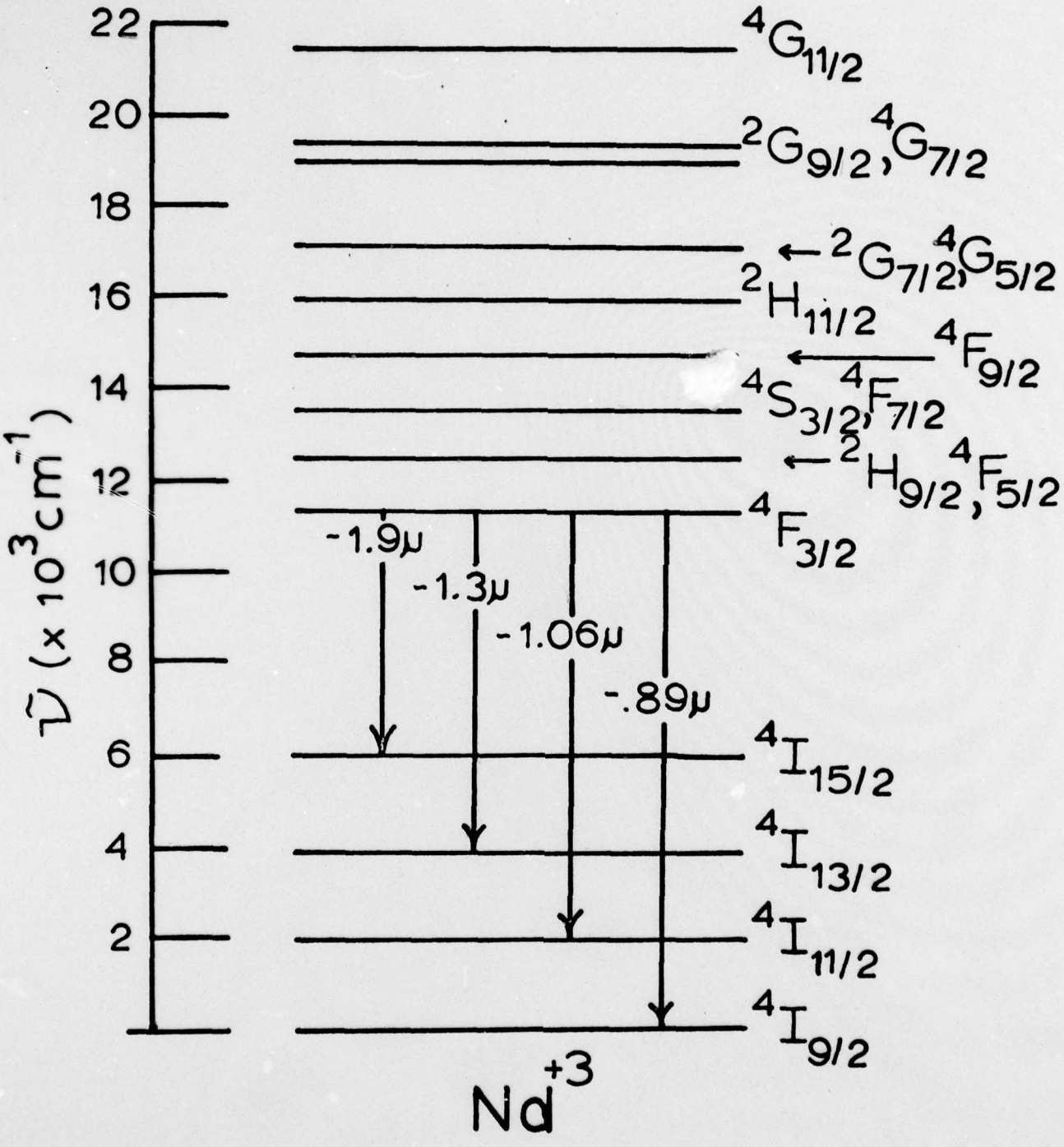
22
20
18
16
14
12
10
8
6
4
2
$\tilde{\nu}$ (x $10^3 cm^{-1}$)
$^4G_{11/2}$
$^2G_{9/2}, ^4G_{7/2}$
$^2G_{7/2}, ^4G_{5/2}$
$^2H_{11/2}$
$^4F_{9/2}$
$^4S_{3/2}, ^4F_{7/2}$
$^2H_{9/2}, ^4F_{5/2}$
$^4F_{3/2}$
-1.9μ
-1.3μ
-1.06μ
-.89μ
$^4I_{15/2}$
$^4I_{13/2}$
$^4I_{11/2}$
$^4I_{9/2}$
Nd^{+3}

Fig. 2

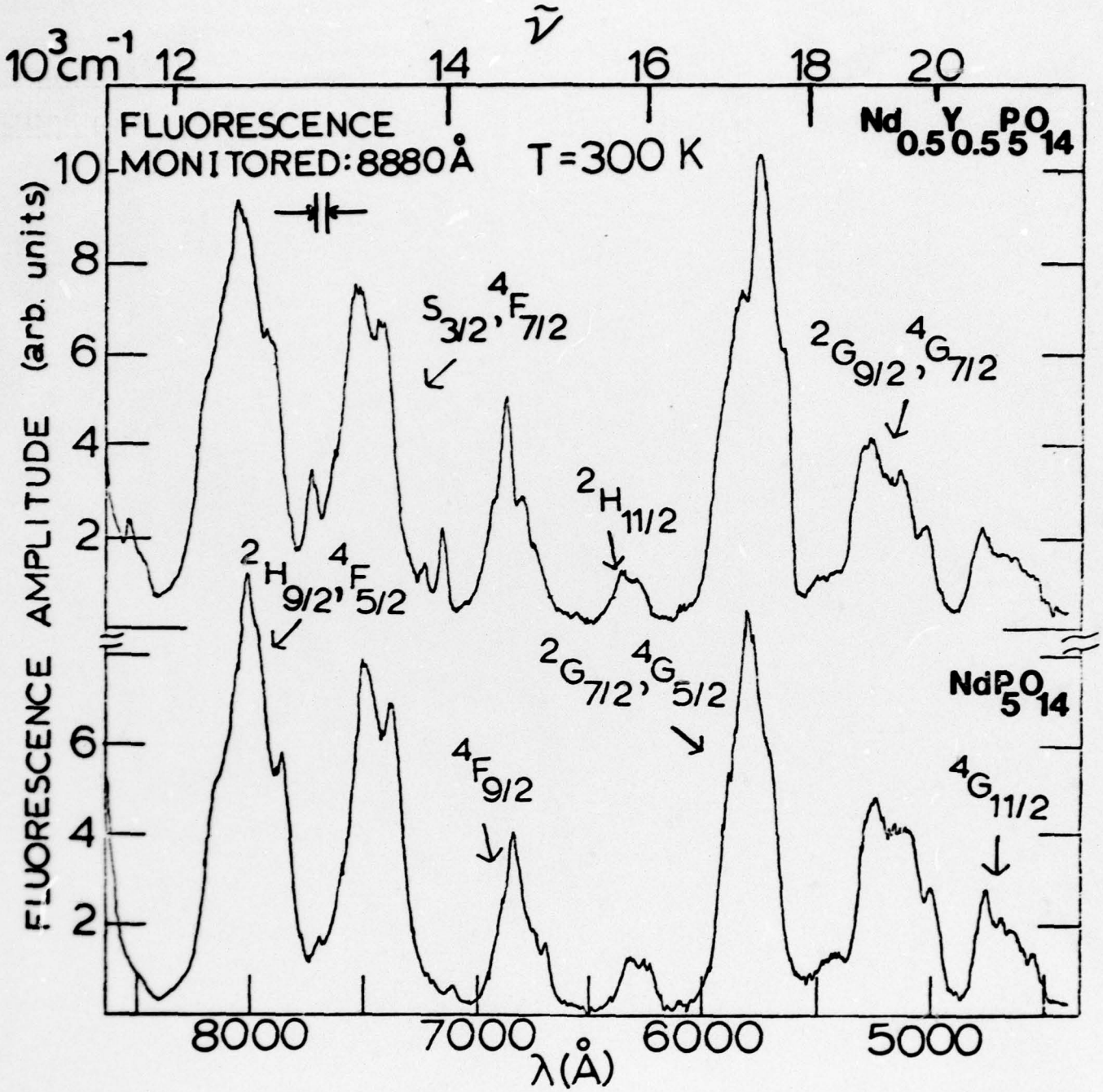
$\tilde{\nu}$
$10^3 cm^{-1}$
12
14
16
18
20
FLUORESCENCE
MONITORED: 8880Å
T = 300 K
$Nd_{0.5}Y_{0.5}P_5O_{14}$
NdP_5O_{14}
FLUORESCENCE AMPLITUDE (arb. units)
$^4S_{3/2}, ^4F_{7/2}$
$^2G_{9/2}, ^4G_{7/2}$
$^2H_{11/2}$
$^2H_{9/2}, ^4F_{5/2}$
$^2G_{7/2}, ^4G_{5/2}$
$^4F_{9/2}$
$^4G_{11/2}$
8000
7000
6000
5000
λ(Å)

Fig. 3

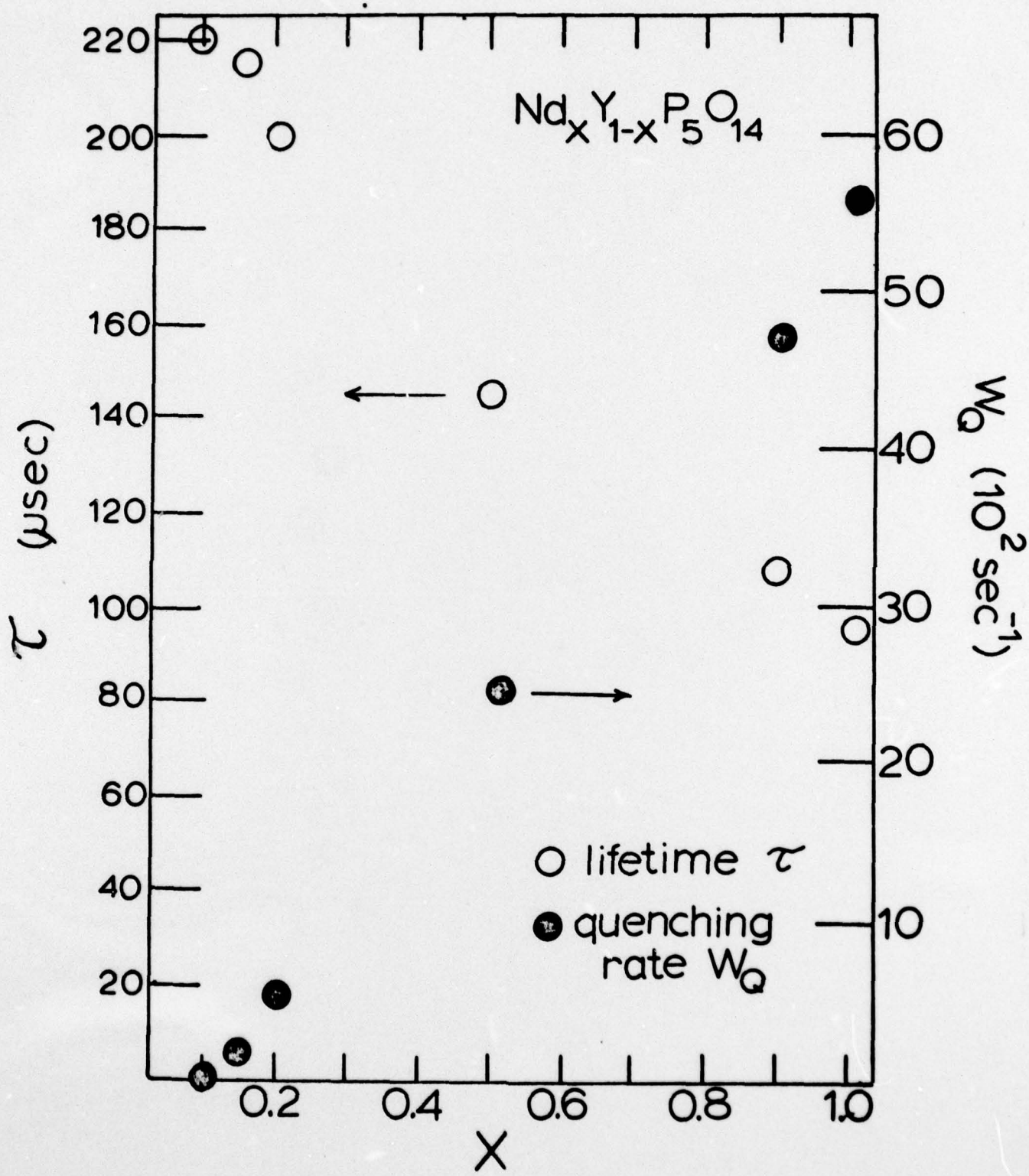
$Nd_xY_{1-x}P_5O_{14}$
τ (μsec)
W_Q (10^2 sec^{-1})
X
220
200
180
160
140
120
100
80
60
40
20
60
50
40
30
20
10
0.2
0.4
0.6
0.8
1.0
O lifetime τ
quenching rate W_Q

Fig. 4

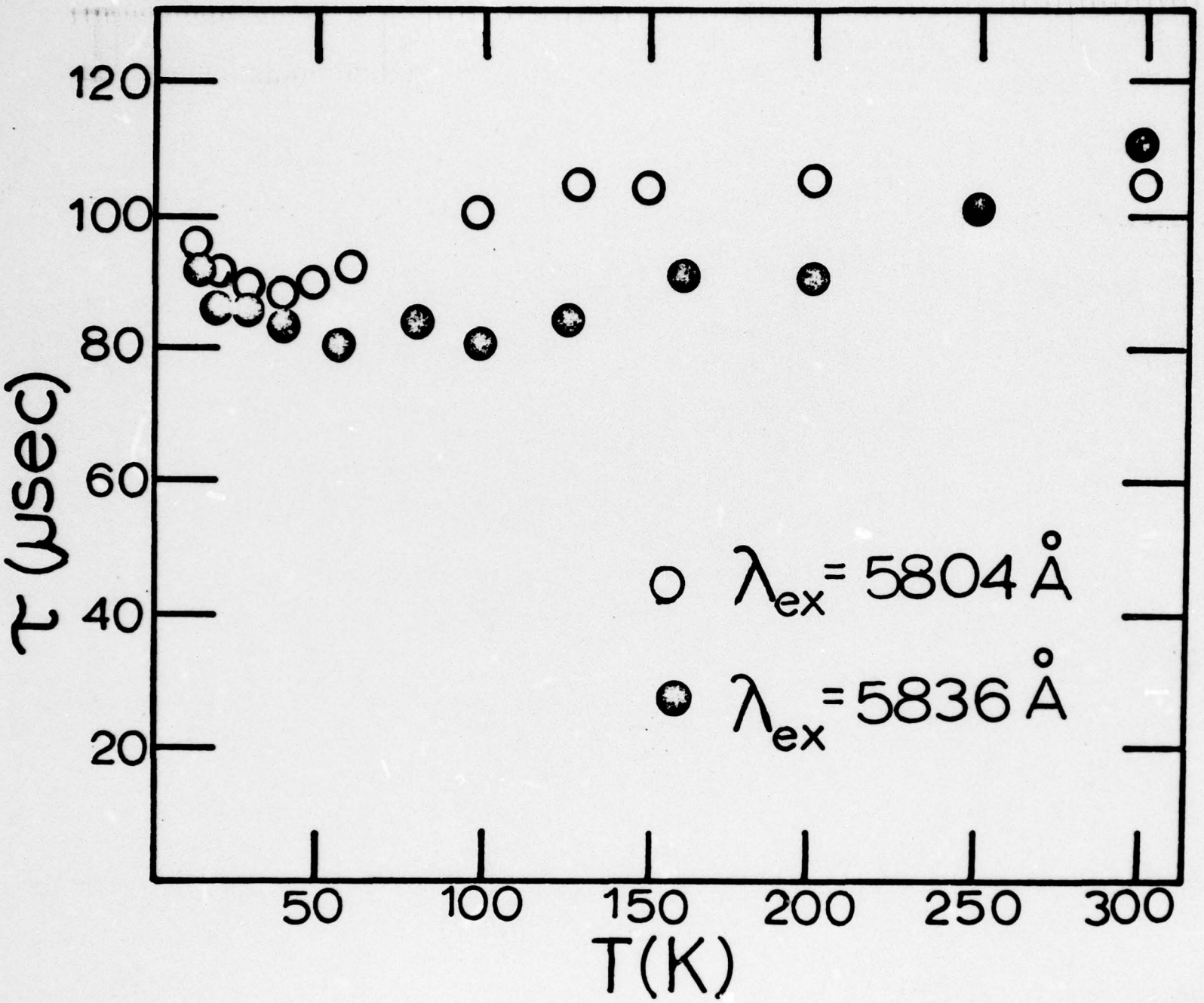
120
100
80
60
40
20
τ (μsec)
50
100
150
200
250
300
T(K)
λex = 5804 Å
λex = 5836 Å

Fig. 5

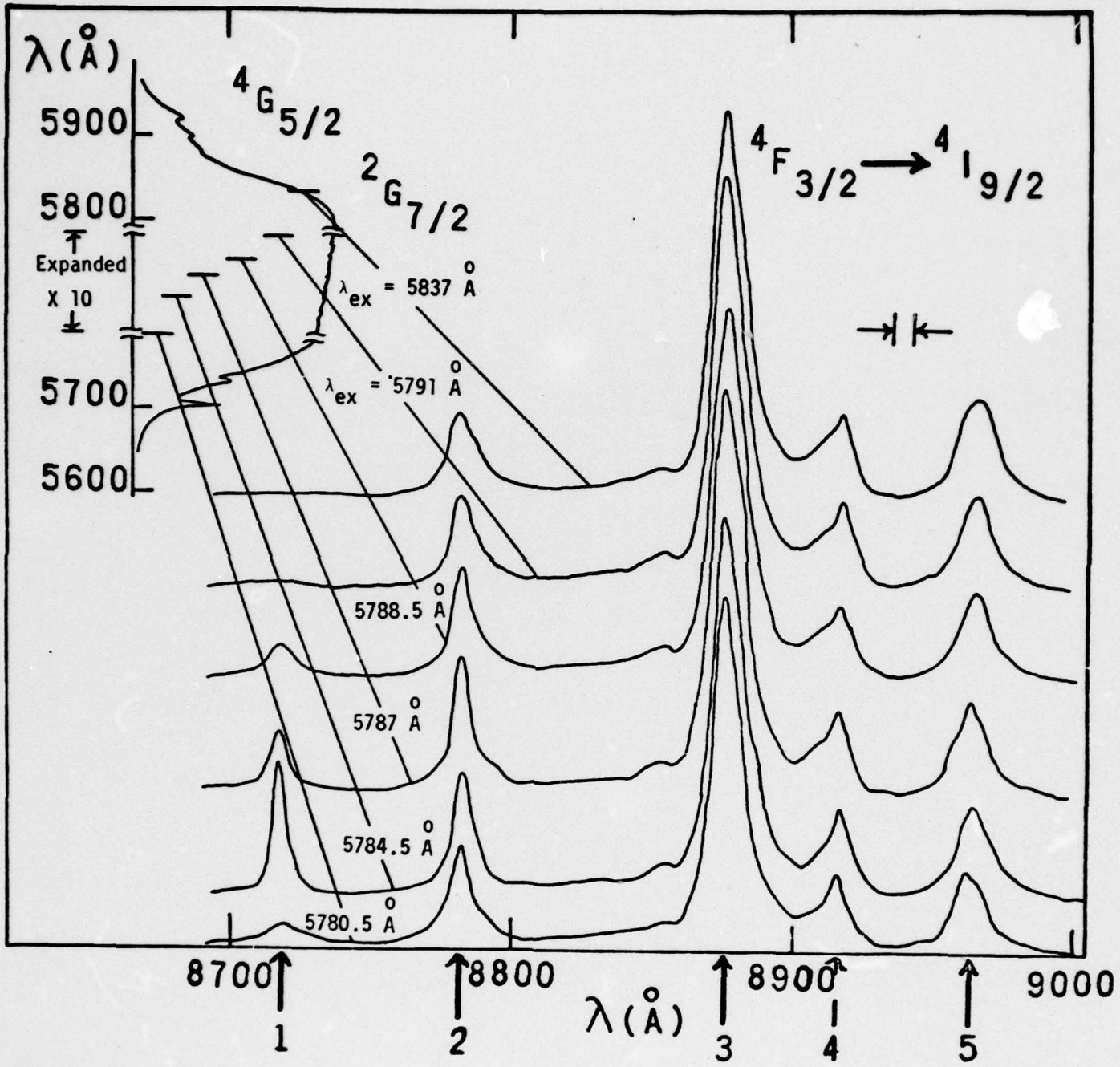
λ(Å)
5900
5800
Expanded
X 10
5700
5600
$^4G_{5/2}$
$^2G_{7/2}$
λ_{ex} = 5837 Å
λ_{ex} = 5791 Å
5788.5 Å
5787 Å
5784.5 Å
5780.5 Å
$^4F_{3/2} \rightarrow {}^4I_{9/2}$
8700
8800
8900
9000
λ(Å)
1
2
3
4
5

Fig. 6

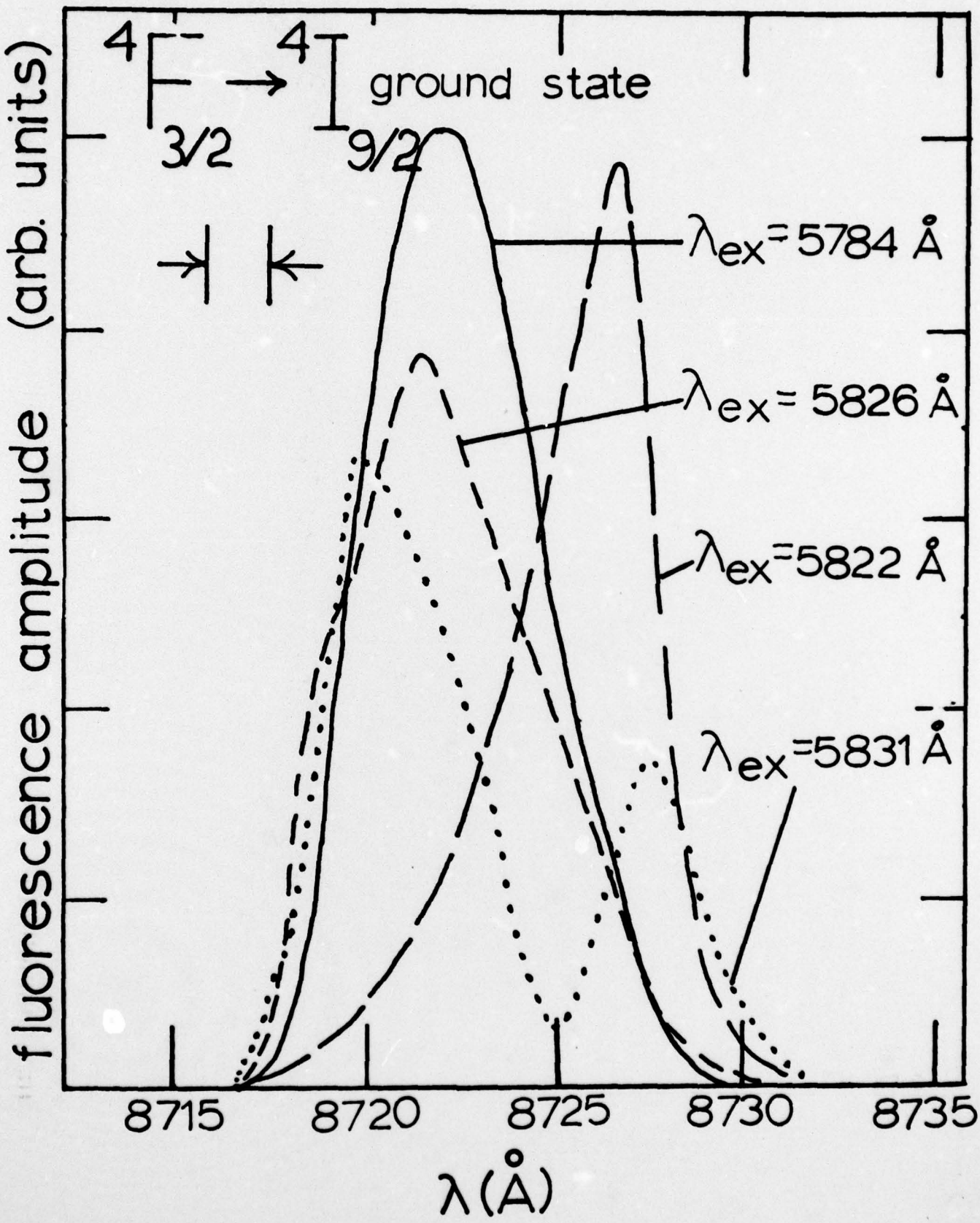
4
4
ground state
3/2
9/2
λ_{ex} = 5784 Å
λ_{ex} = 5826 Å
λ_{ex} = 5822 Å
λ_{ex} = 5831 Å
fluorescence amplitude (arb. units)
8715
8720
8725
8730
8735
λ(Å)

Fig. 7

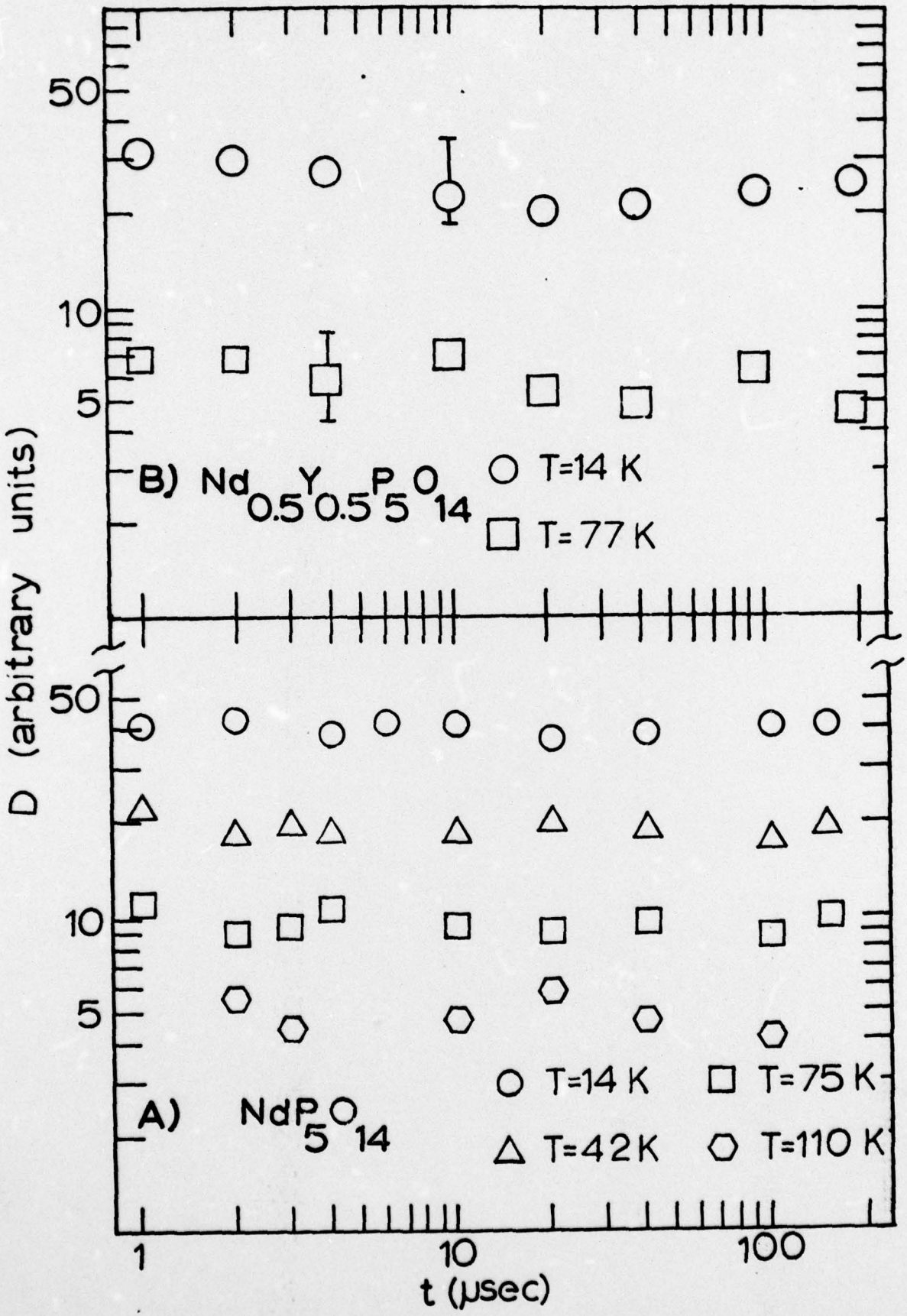
50
10
5
B) $Nd_{0.5}Y_{0.5}P_5O_{14}$
T=14 K
T=77 K
50
10
5
A) NdP_5O_{14}
T=14 K
T=75 K
T=42 K
T=110 K
D (arbitrary units)
1
10
100
t (μsec)

Fig. 8

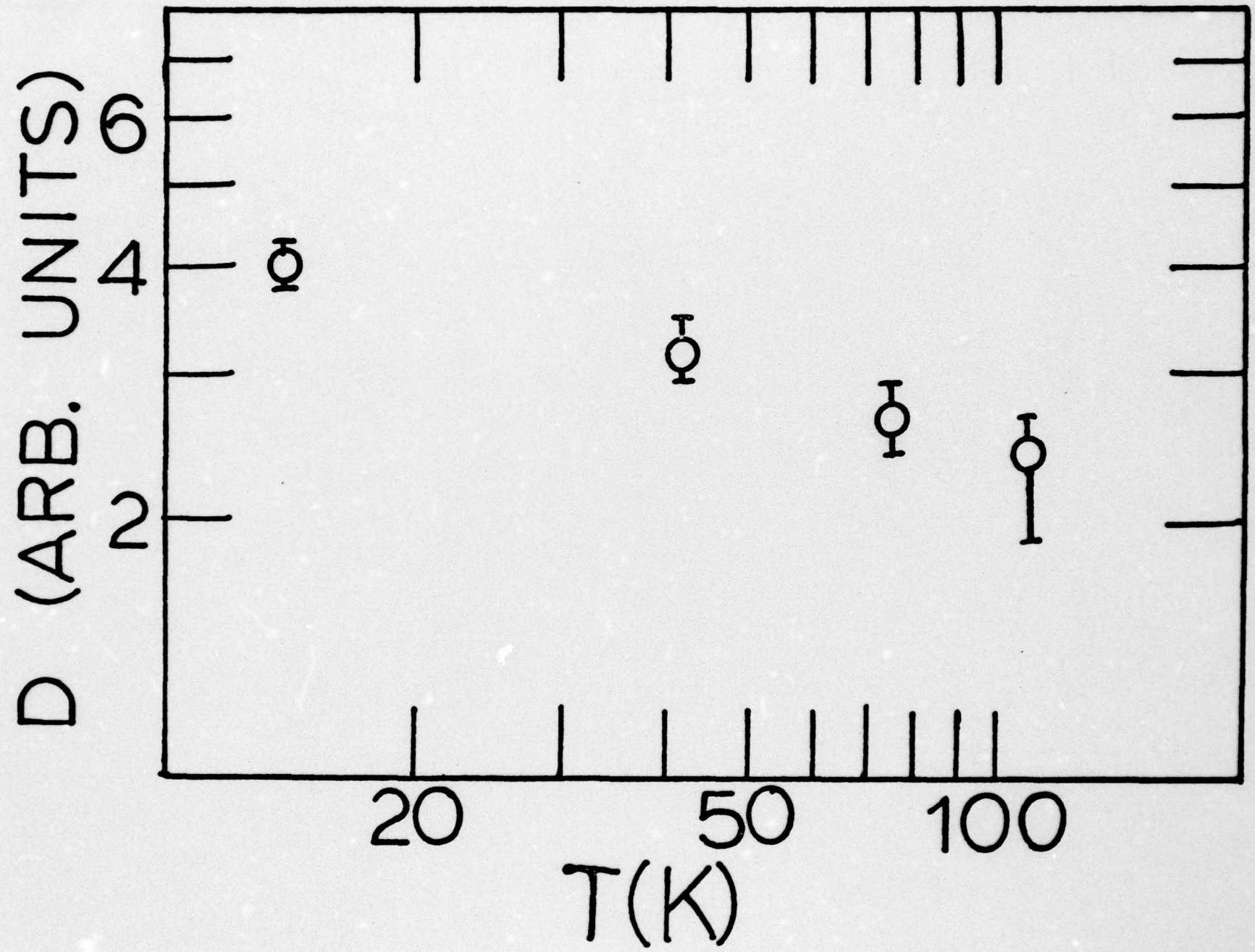

Fig. 10

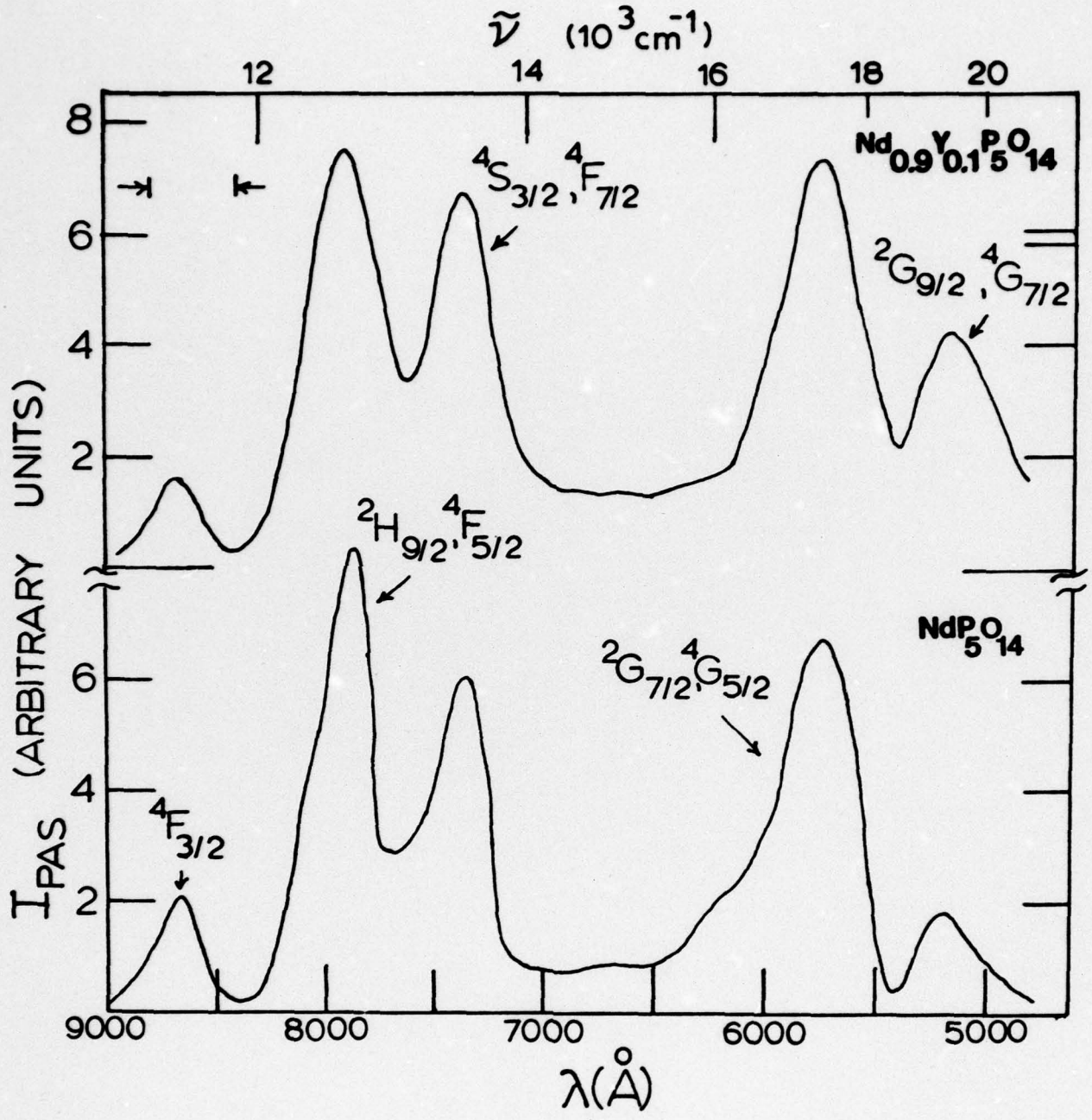
$\tilde{\nu}$ (10^3 cm^{-1})
12
14
16
18
20
8
6
4
2
$^4S_{3/2}$, $^4F_{7/2}$
$^2G_{9/2}$, $^4G_{7/2}$
$Nd_{0.9}Y_{0.1}P_5O_{14}$
$^2H_{9/2}$, $^4F_{5/2}$
$^2G_{7/2}$, $^4G_{5/2}$
NdP_5O_{14}
$^4F_{3/2}$
I_{PAS} (ARBITRARY UNITS)
9000
8000
7000
6000
5000
λ(Å)

Fig. 10

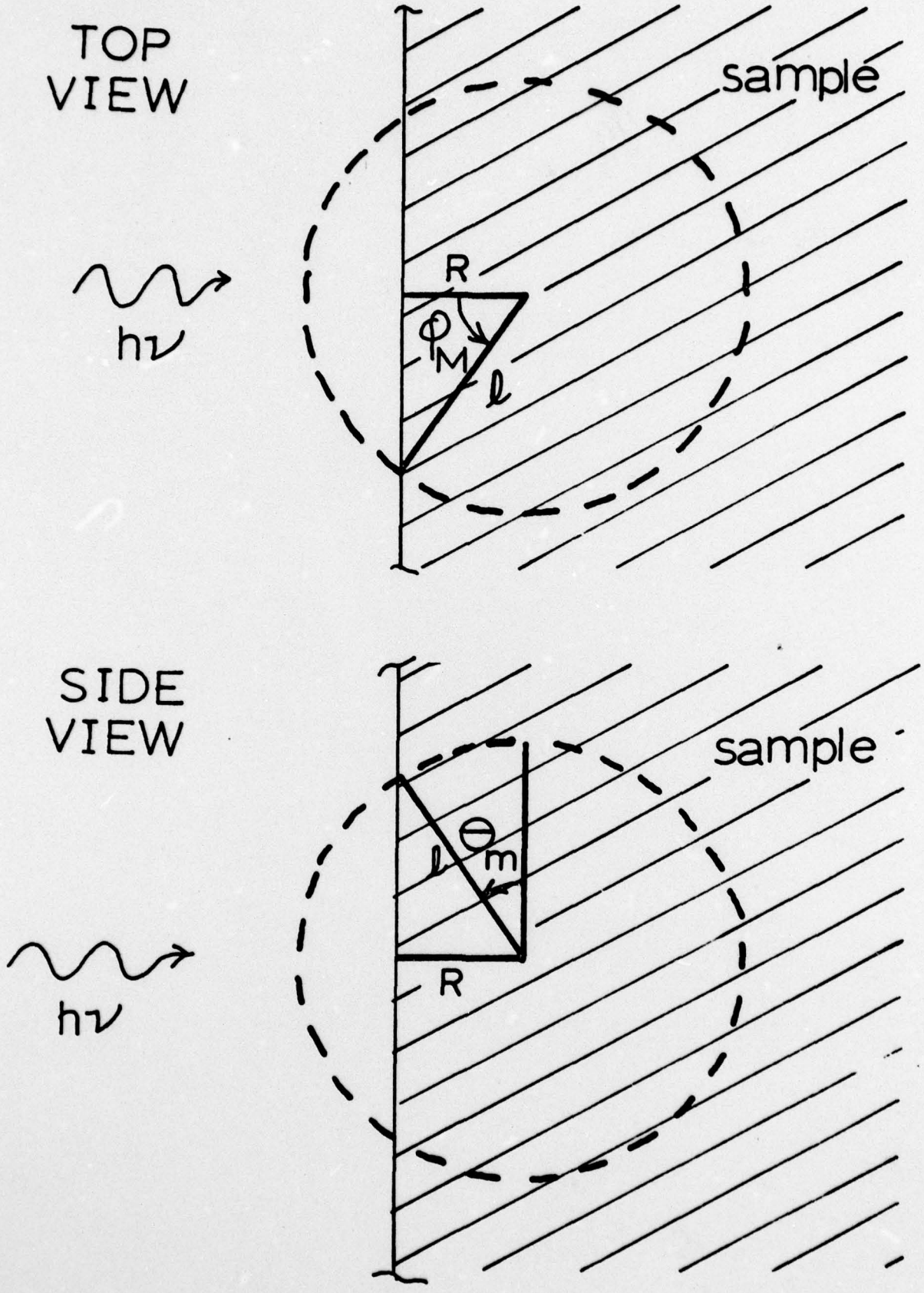

Fig. 11

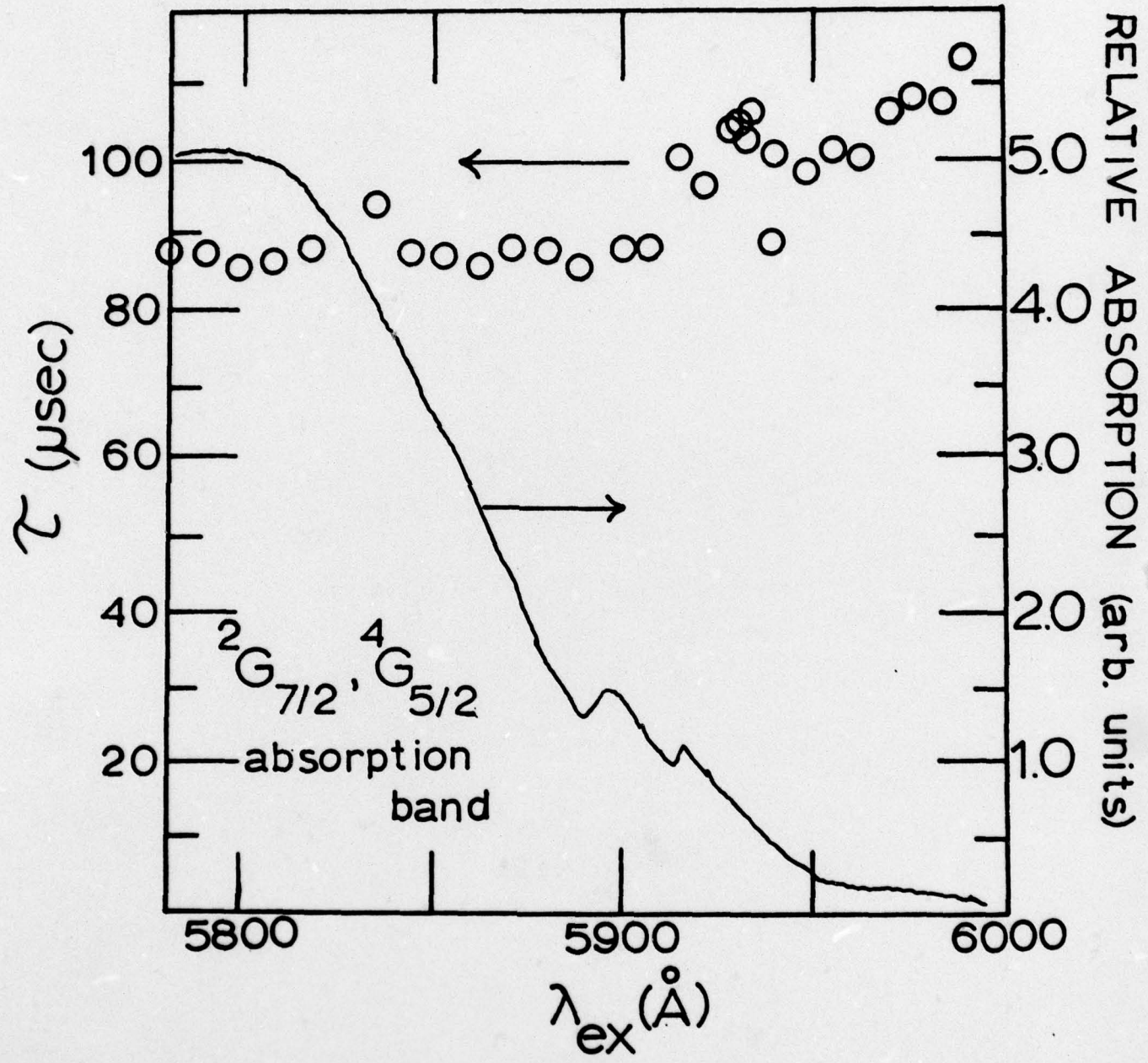
τ (μsec)
100
80
60
40
20
RELATIVE ABSORPTION (arb. units)
5.0
4.0
3.0
2.0
1.0
$^2G_{7/2}$, $^4G_{5/2}$
absorption
band
5800
5900
6000
λ_{ex}(Å)

Fig. 12